

# Four IRAC Sources with an Extremely Red H–[3.6] Color: Passive or Dusty Galaxies at $z > 4.5$ ?

J.-S. Huang<sup>1</sup>, X. Z. Zheng<sup>2</sup>, D. Rigopoulou<sup>3</sup>, and G. Magdis<sup>3</sup>, G. G. Fazio<sup>1</sup>, T. Wang<sup>1,4</sup>

## ABSTRACT

We report detection of four IRAC sources in the GOODS-South field with an extremely red color of  $H-[3.6] > 4.5$ . The four sources are not detected in the deep HST WFC3 H-band image with  $H_{limit} = 28.3$  mag. We find that only 3 types of SED templates can produce such a red H–[3.6] color: a very dusty SED with the Calzetti extinction of  $A_V = 16$  mag at  $z = 0.8$ ; a very dusty SED with the SMC extinction of  $A_V = 8$  mag at  $z = 2.0 \sim 2.2$ ; and an 1Gyr SSP with  $A_V \sim 0.8$  at  $z = 5.7$ . We argue that these sources are unlikely dusty galaxies at  $z \leq 2.2$  based on absent strong MIPS  $24\mu\text{m}$  emission. The old stellar population model at  $z > 4.5$  remains a possible solution for the 4 sources. At  $z > 4.5$ , these sources have stellar masses of  $\text{Log}(M_*/M_\odot) = 10.6 \sim 11.2$ . One source, ERS-1, is also a type-II X-ray QSO with  $L_{2-8keV} = 1.6 \times 10^{44}$  erg  $\text{s}^{-1}$ . One of the four sources is an X-ray QSO and another one is a HyperLIRG, suggesting a galaxy-merging scenario for the formation of these massive galaxies at high redshifts.

*Subject headings:* cosmology: observations — galaxies: evolution — galaxies:formation — infrared: galaxies

## 1. Introduction

Extremely Red Objects(ERO) are of great interests to modern astrophysics. A simple red color criterion generally selects two types of galaxies: those at high redshifts and those with heavy dust extinction. With rapid progress in telescope apertures and detectors, this red color selection always leads to new types of galaxies or galaxies at record-high redshifts. After

---

<sup>1</sup>Harvard-Smithsonian Center for Astrophysics, 60 Garden Str., Cambridge, MA02138, USA

<sup>2</sup>Purple Mountain Observatory, 2 West Beijing Rd., Nanjing, Jiangsu Province, PRC

<sup>3</sup>Department of Physics, Denys Wilkinson Building, Keble Road, Oxford, OX1 3RH, UK

<sup>4</sup>Department of Astronomy, Nanjing University, Nanjing, Jiangsu Province, PRC

large format near-infrared array cameras became available for astronomical surveys, people started to detect galaxies with very red  $R-K$  colors (Elston et al. 1988, EROs,  $R-K > 5$  or  $I-K > 4$ ). EROs were so rare in the early days that they were thought to be abnormal objects at very high redshifts. There have been more and more EROs detected by larger aperture telescopes with more advanced IR array cameras. Most EROs with  $R-K > 5$  are now identified as elliptical and dusty galaxies at  $0.6 < z < 1.5$  (Thompson et al. 1999; McCarthy et al. 2001; Cimatti et al. 2002). One extreme case, an ERO with  $I-K = 6.5$ , was spectroscopically identified as a dusty Ultra-Luminous InfraRed Galaxy (ULIRG) at  $z = 1.44$  (Elbaz et al. 2002). This source is analog to a local ULIRG, Arp220. Smail et al. (2002) suggested that most dusty EROs at high redshifts are LIRG/ULIRGs. The Spitzer IRAC permits very fast imaging of sky in mid-infrared bands with great depth. Wilson et al. (2004) found that 17% of their IRAC  $3.6\mu\text{m}$  selected sample are EROs at  $z \geq 1$ .

Red color criteria are practically diversified, and applied to almost all kinds of photometry in optical and IR bands. But the physics for this type of criteria are limited to following: (1) the Lyman break at  $912\text{\AA}$ ; (2) the Balmer and the accumulated absorption line breaks at  $3648\text{\AA}$  and  $4000\text{\AA}$ ; or (3) dust extinction. Red color caused by the Lyman/Balmer break can be used to estimate redshifts. In most deep broad band imaging surveys, one could not tell if a red color is due to Lyman/Balmer Break or dust extinction (Steidel et al. 2003). An additional color in longer wavelength bands is usually applied together with the red color criterion to select galaxies at high redshifts. For example,  $U-g$  and  $g-R$  colors were used to select galaxies at  $z=3$  where the Lyman break shifts between  $U$  and  $g$  bands, commonly known as  $U$  drop-out for red  $U-g$  color (Steidel et al. 2003). The drop-out technique was applied in much longer wavelength bands to select galaxies at  $z=6\sim 9$ . Franx et al. (2003) used the NIR color  $J-K > 2.3$  to select Distant Red Galaxies (DRGs) with the strong Balmer/ $4000\text{\AA}$  break shifting in between the  $J$  and  $K$  at  $z \sim 2$ . The NIR spectroscopy for DRGs by Kriek et al. (2007) shows that about half of their sample are passive evolved galaxies at  $z \sim 2$ , and the rest are dusty galaxies in a much wider redshift range. Several groups identified  $24\mu\text{m}$  luminous and optically faint or invisible sources with  $R-[24] > 14.2$  ( $f_{24}/f_R > 1000$ ) as very dusty ULIRGs at  $z \sim 2$ . These sources are confirmed spectroscopically by Spitzer IRS and ground-based optical spectroscopy (Houck et al. 2005; Yan et al. 2007; Dey et al. 2008; Huang et al. 2009).

In this paper we report detection of four galaxies with extremely red colors of  $H-[3.6] > 4.5$  in the GOODS-South field. Only one similar source, a submillimeter galaxy (SMG) called GOODS 850-5 (aka GN10) in the GOODS-North field, was ever found to have  $H-[3.6] > 4.5$ . This SMG was also detected by the Submillimeter Array (Wang et al. 2007) with a high angular resolution of  $\sim 2''$ , permitting identification of its counterparts in shorter wavelength bands. Wang et al. (2009) performed ultra-deep  $J$  and  $H$  band imaging for this source with

NIC3 camera on HST. A total of 16 orbits of HST observation, reaching a nanoJansky depth in the F160W band, yields no detection for this source. Based on this red  $H-[3.6]$  color, they argue that its redshift is at  $z=4\sim 6.5$ . Later, detection of CO(4-3) from this source confirms its redshift at  $z=4.05$  (Daddi et al. 2009). This study provides the first look at properties of this new type of object. More sources of this kind will be detected in the Cosmic Assembly Near-infrared Deep Extragalactic Legacy Survey (Grogin et al. 2011, CANDELS).

## 2. Deep IR Imaging of GOODS-South

The Great Observatories Origins Deep Survey (GOODS) is the deepest multi-wavelength survey with space telescopes including HST, Spitzer and Chandra (Dickinson 2004). The depth of GOODS IRAC  $3.6\mu\text{m}$  imaging reaches sub-microJansky level. The deep NIR imaging of the GOODS-South field was selected for the Early Released Science (O’Connell 2010, ERS) for the Wide Field Camera 3 (WFC3), a fourth-generation UVIS/IR imager aboard HST. We construct an H-selected multi-wavelength catalog including YJH+IRAC photometry in the ERS covered region. The IR images have very different angular resolutions:  $0.03''$  for the HST WFC3 YJH band images and  $\sim 2''$  for the Spitzer IRAC  $3.6\text{--}8.0\mu\text{m}$  images. A photometry program called TFIT is specifically designed to perform photometry on a lower resolution image with input information of object positions and light distributions measured in a high resolution image (Laidler et al. 2007). The TFIT program convolves a PSF kernel to the high angular resolution stamp image for each object to construct lower angular resolution image templates and fit them to the lower angular resolution image. In our case, we ran the TFIT to perform photometry on the IRAC  $3.6\mu\text{m}$  image for the H-band selected galaxies detected in the ERS F160W image. The TFIT also produces a residual image after subtracting all H-band detected galaxies in the  $3.6\mu\text{m}$  image. We visually inspected the residual image and found four IRAC sources detected at  $3.6\mu\text{m}$  with no H-band counterparts shown in Figure 1. The limiting magnitude for the input H-selected sample is  $H=28.3$  mag at  $3\sigma$  level, therefore these sources are fainter than  $H=28.3$  mag and have colors redder than  $H-[3.6]=4.5$ .

We searched for counterparts of these sources in all available wavelength bands in the GOODS-South field. All four sources are detected in the remaining 3 IRAC bands. None of these sources is detected in the GOOD-South ACS BVIZ images with the  $5\sigma$  limiting magnitudes of 28.65, 28.76, 28.17, and 27.93 respectively. The K-band is the only band available in between H and  $3.6\mu\text{m}$ , permitting further constraint on its SED and photometric redshift. The  $5\sigma$  limiting magnitude for the K-band image of the GOOD-South field (Retzlaff et al. 2010) is 24.4 mag and none of our sources is detected in K band. FIR observation is also

critical in determining properties of these red sources (Wang et al. 2009). ERS-3 is clearly detected at  $24\mu\text{m}$  and ERS-2 is marginally detected at  $\sim 3\sigma$  level. We inspected the Herschel SPIRE deep imaging of the CDFS, and found only ERS-3 is marginally detected at  $250\mu\text{m}$  and  $350\mu\text{m}$ . The PSF for the SPIRE  $500\mu\text{m}$  band image is too broad ( $36.6''$ ) to permit accurate extraction of flux density for ERS-3 (Huang et al. 2011). ERS-3 is also detected at  $1.4\text{GHz}$  with  $f_{1.4\text{GHz}}=29.2\pm 8\mu\text{Jy}$ . The remaining three sources are not detected in radio with  $f_{1.4\text{GHz}} < 24\mu\text{Jy}$ . No submillimeter/millimeter source is detected in the locations of these four sources (Scott et al. 2009; Weiß et al. 2009). Another source, ERS-1, is an X-ray source in the Chandra 2Ms catalog (Alexander et al. 2003). ERS-2 and ERS-4 are detected only in 4 IRAC bands (Table.1).

### 3. SEDs, Photometric Redshifts, and Properties of the Extremely Red Objects

For three out of the four sources in this study, only NIR+IRAC flux densities are available for their photometric redshift estimation. The most predominant feature in their SEDs is the extremely red color of  $H-[3.6]>4.5$ . We first rule out that those sources are brown dwarves. A brown dwarf with  $T=600\text{K}$  has  $H-[4.5]>4.0$  (Legget et al. 2010), such a brown dwarf should have  $[3.6]-[4.5]>1$  due to the methane absorption at  $3.6\mu\text{m}$  in its photosphere. All our sources have  $[3.6]-[4.5]<0.5$ . It is unlikely that this red color is due to the Lyman break at  $z>15$ . Galaxies with a strong Balmer/ $4000\text{\AA}$  break at  $3<z<8$  can have very red  $H-[3.6]$  colors. Recently Richard et al. (2011) detected a lensed source at  $z=6.02$  behind cluster A383 with  $H-[3.6]=1.5$ , arguing that this is a possible passive galaxy. A few more lensed galaxies with extreme red optical-MIR color are identified to be dusty galaxies at either  $z\sim 2$  or  $z>6$  (Boone et al. 2011; ?). Their  $H-[3.6]$  colors are only in range of  $0.5<H-[3.6]<2$ .

#### 3.1. SED Fitting

We model the  $H-[3.6]$  color using stellar population models of both BC03 (Bruzual & Charlot 2003, BC03) and the upgraded model CB07 (Charlot & Bruzual 2007) emphasizing on AGB star contribution in the rest-frame NIR bands. The templates are constructed with various stellar populations of the solar metallicity and a very wide range of dust extinction of  $0<A_V < 25$ . The star formation history used in constricting the template set includes single burst, exponential decreasing with various e-fold times, and constant rates. Two types of extinction curves are used in the SED templates: the widely used Calzetti extinction curve

for galaxies (Calzetti et al. 2000) and the SMC extinction curves (Gordon et al. 2003). Both extinction curves are only up to  $2.2\mu\text{m}$ , while our detected photometry points for the four sources are in  $3.6 < \lambda < 8.0\mu\text{m}$ . We extend both curve to the IRAC bands using the MIR dust extinction curve in  $3.6 < \lambda < 24\mu\text{m}$  (Chapman et al. 2009).

We first fitted our model templates to GOODS 850-5 to investigate what kind of stellar population and how much amount of dust extinction can make such a red H–[3.6] color. GOODS 850-5 is already known at  $z=4.05$ , thus provides better constraint on stellar population and dust extinction. Both BC03 and CB07 models with either Calzetti or SMC extinction yields a similar result for GOODS 850-5 : 1Gyr old single stellar population with modest extinction of  $A_V=2.4\sim 3.6$ . The best fit template is an 1Gyr single stellar population model with the Calzetti extinction of  $A_V=3.6$ . Wang et al. (2009) obtained a similar model template for their best fitting but yielding much higher redshifts at  $z=6.9$ .

We argue that the four objects in this study are at the same redshifts: they have very similar SEDs, and their positions are very close to each other, with a mean distance of  $\sim 1.5'$  to their closest neighbors. We fitted the SED templates to the six IR photometry points (H, K, and 4 IRAC bands) for each object in the sample. Our fitting yields two extreme solutions with the Calzetti extinction: a very dusty template with  $A_V=16\sim 18$  at  $z\sim 0.8$  and an old stellar population template with  $z\sim 5.7$  and  $A_V\sim 0.8$  (Figure 2). The templates with the SMC extinction yields a similar dusty solution with  $A_V=7\sim 8$  at  $z\sim 2.2$ . By applying heavy dusty extinction with  $A_V > 7$  to templates, its shape and the resulting photometric redshift are only determined by extinction curves. For example, the SMC extinction curve yields a photometric redshift of  $z_p=2.2$  for our objects, which is caused by a dip at  $1.25\mu\text{m}$  in the SMC extinction curve ( $A(1.65\mu\text{m})/A_V=0.169$ ,  $A(1.25\mu\text{m})/A_V=0.131$ , and  $A(0.81\mu\text{m})/A_V=0.567$ , Gordon et al. (2003)). With a very high  $A_V$  value, this feature is amplified. At  $z=2.2$ , this extinction dip shifts to the IRAC  $3.6\mu\text{m}$  band to make H–[3.6] redder and [3.6]–[8.0] bluer. The photometric redshifts obtained with the SMC extinction curve are mainly driven by this feature.

There are generally three final solutions (Figure 2) in our SED fitting for the 4 objects: a dusty template at  $z=0.8$  with the Calzetti extinction of  $A_V=16$ ; a dusty template at  $z=2.2$  with the SMC extinction of  $A_V=8$ ; and an old stellar population template with age of 1Gyr and  $A_V < 1$ . Though each solution has a slightly different minimum  $\chi$  of  $3 < \chi_{min} < 6$ , we consider each solution equally possible. All three SED models are able to produce H–[3.6] $>4.5$ , and require extreme conditions in the galaxies: either extremely dusty of  $A_V > 7$  or even  $A_V=16$  or very massive galaxies at  $z>4.5$ , both of which are very rare in current extragalactic surveys.

### 3.2. Extremely Dusty Galaxies at $z < 3$ ?

In the first solution, a galaxy with the Calzetti extinction of  $A_V \sim 16$  at  $z=0.8$  can have  $H-[3.6] > 4.5$ . At  $z=0.8$ , the IRAC  $3.6\mu\text{m}$  band probes the rest-frame K-band. Our sources have  $3.6\mu\text{m}$  flux density of  $f_{3.6}=0.6\sim 1.5\mu\text{Jy}$ , implying that their stellar masses are less than  $5 \times 10^9 M_\odot$ . Most galaxies with such a small stellar mass at  $z=0.8$  are blue galaxies with no dust extinction. M82 is a dusty galaxy with lower stellar mass of  $4 \times 10^9 M_\odot$ , with heavy dust obscuration ( $5 < A_V < 51$ ) only occurring in its center (Beirão et al. 2008). The whole M82 appears much bluer than our objects. The  $H-[3.6]$  color at  $z=0.8$  is equivalent to the rest-frame I–K color. M82 has  $I-K=0.82$  (Dale et al. 2007), because most stars in the disk of M82 are in the outside of its dusty region. Thus an object like M82 at  $z=0.8$  would be detected in the ERS H-band imaging. This solution, however, requires that the whole galaxy should be in heavy obscuration. Only ULIRGs have such a obscured morphology. Using M82 central region SEDs, we predict that the MIPS  $24\mu\text{m}$  flux densities for the first 3 sources would have  $f_{24}=50\sim 70\mu\text{Jy}$ , well above the FIDEL MIPS  $24\mu\text{m}$  limiting flux density. Only ERS3 is marginally detected at  $24\mu\text{m}$  with  $f_{24}=39\mu\text{Jy}$ , the rest are not detected at  $24\mu\text{m}$ . We argue that this scenario is least possible.

The second solution is the template with the SMC extinction of  $A_V=7\sim 8$  at  $z=2\sim 2.2$ . There are many Dust Obscured Galaxies(DOG) identified at  $z\sim 2$  (Houck et al. 2005; Dey et al. 2008; Bussmann et al. 2009). Several groups (Houck et al. 2005; Yan et al. 2007; Huang et al. 2009) performed mid-infrared spectroscopy for DOGs and detected a very strong silicate absorption feature at  $9.8\mu\text{m}$  in their spectra, indicating a very heavy dust extinction. Bussmann et al. (2009) took high resolution H-band imaging of these sources in the Bootes field with NICMOS on HST to study their rest-frame optical morphologies. We identified these DOGs in the Bootes IRAC photometry catalog (Ashby et al. 2009), and found that DOGs were generally red with  $1.5 < H-[3.6] < 3.3$ , and luminous at  $3.6\mu\text{m}$  with  $f_{3.6}=5\sim 60\mu\text{Jy}$ . The four sources in this study are much fainter at  $3.6\mu\text{m}$ , and have a much redder color of  $H-[3.6] > 4.5$ . On the other hand, the DOGs in Bussmann et al. (2009) have a 24-to- $8\mu\text{m}$  flux ratio of  $f_{24}/f_8=40\sim 350$ . If the 4 sources were indeed fainter DOGs at  $z\sim 2$ , they should have a  $24\mu\text{m}$  flux density of  $f_{24} > 120\mu\text{Jy}$ , much higher than the  $24\mu\text{m}$  limiting flux density in GOODS-South. Based on much redder  $H-[3.6]$  and fainter  $24\mu\text{m}$  flux, we argue that these objects are at higher redshifts than the DOGs at  $z\sim 2$ .

### 3.3. Massive Galaxies at $z > 4.5$ ?

The 1Gyr SSP template with the Calzetti extinction of  $A_V=0.8$  at  $z\sim 5.7$  can also fit the SEDs of the four objects, very similar to the best-fit template for GOODS 850-5. In this

scenario, the red H–[3.6] is mainly due to the Balmer/4000Å jump shifting in between H and 3.6μm bands at  $z > 4$ . Figure 3 shows that the old stellar template fits to SEDs of the 4 objects. The resulting photometric redshifts have a large error of  $0.4 < \sigma(z) < 1.1$ . We argue that the 4 objects are at the same redshifts. Thus by adopting the best  $\sigma(z)$  in the 4 objects, these objects should be at  $z > 4.5$  at  $3\sigma$  level.

ERS-3 is detected at 250 and 350μm, thus has a very strong FIR emission, very similar to GOODS 850-5 (Huang et al. 2011). The best fit SED models for both GOODS 850-5 and ERS-3 are old stellar population models. We propose a two-component SED model to reconcile the old stellar population and FIR emission in these objects: an old stellar population and a very dusty star-forming component. The star-forming component is so dusty, similar to those dusty galaxies detected at  $z \sim 2$  (Houck et al. 2005; Yan et al. 2007; Dey et al. 2008; Huang et al. 2009), that its optical/NIR SED is dominated by the old stellar population component. For example, a dusty component with the same stellar mass and  $A_V = 6$  at  $z > 5$  would only contribute 10% increase at 8 micron, and much lower percentage in the shorter IRAC bands. Assuming a typical dust temperature of  $T_{dust} = 40\text{K}$  and redshift of  $z = 5.7$ , we calculate the FIR luminosity for ERS-3 as  $\text{Log}(L_{FIR}/L_{\odot}) = 13.1$ . The FIR-to-Radio flux ratio is about  $q = 2.26$ , consistent with  $q$  values for submillimeter galaxies at  $z > 4$  (Huang et al. 2011). The remaining 3 objects are not detected by Herschel SPIRE, but may still be IR luminous galaxies with just  $\text{Log}(L_{FIR}/L_{\odot}) < 13.1$ .

The SSP model fitting also yields stellar mass of  $\text{Log}(M_*/M_{\odot}) = 10.6 \sim 11.2$  for our sources (Figure 3). Spectroscopic confirmed galaxies at  $z \sim 5.7$  including both Lyman-break (LBGs) and Ly- $\alpha$  (LAE) galaxies have a typical stellar mass of  $\text{Log}(M_*/M_{\odot}) \leq 10$  (Yan et al. 2006; Lai et al. 2007; Younger et al. 2007; Richard et al. 2011). Recently Marchesini et al. (2010) argued that very massive galaxies were already formed at  $3 < z < 4$ . Theoretically, Li et al. (2007) argued that QSOs at  $z > 6$  resided in a massive halo of  $M \sim 8 \times 10^{12} M_{\odot}$ , and stellar mass for their host galaxies can be as high as  $10^{12} M_{\odot}$ . We have another piece of evidence consistent with these systems being massive. ERS-1 is also an X-ray source detected in the Chandra 2Ms survey (Alexander et al. 2003). It has x-ray flux densities of  $f_{0.5-2keV} = 7.55 \pm 2.14 \times 10^{-17} \text{erg s}^{-1} \text{cm}^{-2}$  and  $f_{2-8keV} = 6.50 \pm 1.50 \times 10^{-16} \text{erg s}^{-1} \text{cm}^{-2}$ . The hard X-ray Luminosity for this source is  $L_{2-8keV} = 1.6 \times 10^{44} \text{erg s}^{-1}$  at  $z_p = 5.7$  assuming no absorption correction. Its X-ray-to-optical-flux ratio ( $f_x/f_R$ ) is higher than 60 and the hardness ratio is  $\sim 1$ , thus ERS-1 is an obscured type-II QSO. A typical black hole mass for such a QSO at  $z = 3 \sim 6$  is  $10^9 \sim 10^{10} M_{\odot}$  (Netzer 2003; Shemmer et al. 2004; Fan et al. 2006). Assuming a typical H $\alpha$  FWHM of 2000 km/s for a QSO, we convert the  $L_{2-8keV}$  to black hole mass for ERS-1 as  $M_{BH} = 5 \times 10^8 M_{\odot}$  using the relation proposed by Sarria et al. (2010). Trakhtenbrot & Netzer (2010) argued that a host galaxy with  $10^9 M_{\odot}$  black hole has a typical stellar mass of  $M_* \sim 10^{11} M_{\odot}$ , consistent with the stellar mass we derived for

ERS-1.

#### 4. Summary and Discussion

We identified four IRAC sources in the GOODS-South field with extremely red color of  $H-[3.6]>4.5$ . The only known source with a similar  $H-[3.6]$  color is GOODS 850-5, a SMG in the GOODS-North field. We argue that the four sources must be at the same redshift based on the following facts: they have similar rest-frame optical/NIR SEDs; and they are spatially very close to each other with a mean angular distance  $\sim 1.5'$ . Only 3 types of templates can produce  $H-[3.6]>4.5$ : a very dusty template with the Calzetti extinction of  $A_V=16$  mag at  $z=0.8$ ; a very dusty templates with the SMC extinction of  $A_V=8$  mag at  $z=2.0$ ; and an 1Gyr SSP model with  $A_V \sim 0.8$  at  $z=5.7$ . By comparing the 4 objects with local dusty galaxies and DOGs at  $z\sim 2$ , we argue that they are unlikely dusty galaxies at  $z=0.8$  or  $z=2.2$  based on absent strong  $24\mu\text{m}$  emission. The old stellar population model at  $z>4.5$ , with the best fit at  $z=5.7$ , remain a possible solution for the 4 sources. One of our sources, ERS-3, is also detected by Herschel at  $250\mu\text{m}$  and  $350\mu\text{m}$ , yielding  $\text{Log}(L_{FIR}/L_\odot)=13.2$ . We propose a two-component SED model for these sources: an old SSP component dominating their optical-to-MIR SEDs and a very dusty star-forming component mainly contributing to their FIR SEDs. The SED fitting yields stellar masses of  $\text{Log}(M_*/M_\odot)=10.6\sim 11.2$  for the four sources. One source, ERS-1, is also a type-II x-ray QSO with  $L_{2-8keV}=1.6\times 10^{44} \text{erg s}^{-1}$ . Based on the  $M_{BH}-M_{bulge}$  relation for high- $z$  QSOs, ERS-1 should have a massive bulge of  $\text{Log}(M_*/M_\odot)=11$ . One of the four sources is an X-ray QSO and another one is a HyperLIRG, suggesting a galaxy-merging scenario for the formation of these massive galaxies at high redshifts.

This work is based on observations made with the *Spitzer Space Telescope*, which is operated by the Jet Propulsion Laboratory, California Institute of Technology under NASA contract 1407, and with the NASA/ESA HST obtained at the Space Telescope Science Institute, which is operated by the association of Universities for Research in Astronomy, Inc., under NASA contract NAS 5-26555.

Facilities: Spitzer(IRAC), HST(STIS), CXO(ASIS).

#### REFERENCES

Alexander, D. M. et al. 2003, AJ, 126, 2

- Ashby, M. L. N. et al. 2009, ApJ, 701, 428
- Beirão, P. et al. 2008, ApJ, 676, 304
- Bruzual, G. & Charlot, S. 2003, MNRAS, 344, 1000
- Boone, F., et al. 2011, A&A, in press
- Bussmann, R. S., et al. 2009, ApJ, 693,750
- Calzetti, D. et al. 2000, ApJ, 533, 682
- Charlot, S & . Bruzual, G. Private Communication
- Chapman, N. et al. 2009, ApJ, 690, 496
- Cimatti, A. et al. 2002, A&A, 381,68
- Dey, A. et al. 2008, ApJ, 667, 943
- Daddi,E., Dannerbauer,H., Krips,M., Walter,F., Dickinson,M., Elbaz,D., & Morrison,G.E.  
2009, ApJ, 695, 176
- Dale, D. A. et al. 2007, ApJ, 655, 863
- Dickinson, M. 2004, AAS, 20516301
- Elbaz, D. et al. 2002, A&A, 381, 1
- Elston, R., Rieke, G. H., & Rieke, M. J. 1988, ApJ, 331,71
- Fan,X., Strauss,M.A., Becker,R.H., White,R.L., Gunn,J.E., Knapp,G.R., Richards,G.T.,  
Schneider,D.P., Brinkmann,J., & Fukugita,M. 2006, AJ, 132, 117
- Franx, M. et al. 2003, ApJ, 587, 79
- Gordon, K. et al. 2003, ApJ, 594, 279
- Grogin, N. et al. 2011, in preparation.
- Houck, J. et al. 2005, ApJ, 622, 105
- Huang, J.-S. et al. 2009, ApJ, 700,183
- Huang, J.-S. et al. 2011, submitting to ApJ
- Kriek, K. et al. 2007, ApJ, 669, 776

- Lai,K., Huang,J.-S., Fazio,G. G., Cowie,L.L., Hu,E.M., Kakazu,Y. 2007, ApJ, 657, 704
- Laidler,V.G., Papovich,C., Grogin,N.A., Idzi,R., Dickinson,M., Ferguson,H.C., Hilbert,B.,  
Clubb,K., Ravindranath,S. 2007, PASP, 119,1325
- Laporte, N., et al. 2011, A&A, 531, 74
- Legget, S. K. et al. 2010, ApJ, 710,1672
- Li, Y. et al. 2007, ApJ, 665, 187
- Marchesini, D. et al. 2010, ApJ, 725, 1277
- McCarthy, P. et al. 2001, ApJ, 560, 131
- Netzer, H. 2003, ApJ, 583, 5
- O’Connell,R.W. 2010, AAS, 21522205
- Retzlaff,J., Rosati,P., Dickinson,M., Vandame,B., Rite,C., Nonino,M., Cesarsky,C., GOOD-  
STeam, 2010, A&A, 511, 50
- Richard, J., Kneib, J.-P., Ebeling, H., Stark D. P., Egami, E., & Fiedler, A. K. 2011,  
MNRAS, in press
- Sarria,J.E., Maiolino,R., LaFranca,F., Pozzi,F., Fiore,F., Marconi,A., Vignali,C., & Comas-  
tri,A. 2010, A&A, 522, 3
- Scott, K. S. et al. 2009, MNRAS, 405, 2260
- Shemmer,O., Netzer,H., Maiolino,R., Oliva,E., Croom,S., Corbett,E., & diFabrizio,L, 2004,  
ApJ, 614, 547
- Smail, I. et al. 2002, ApJ, 581, 884
- Steidel, C. C., Adelberger, K. L., Shapley, A. E., Pettini, M., Dickinson, M., & Giavalisco,  
M., 2003, ApJ, 592, 728
- Thompson, et al. 1999, ApJ, 523,100
- Trakhtenbrot, B. & Netzer, H. 2010, MNRAS, 406, 35
- Wang,W.-H., Cowie,L.L., vanSaders,J., Barger,A.J., & Williams,J.P. 2007, ApJ, 670,89
- Wang,W.-H., Barger,A.J., Cowie,L.L. 2009, ApJ, 690, 319

Weiβ, A. et al. 2009, ApJ, 707, 1201

Williams, R.J., Quadri, R.F., Franx, M., van Dokkum, P., Toft, S., Kriek, M., & Labbe, I., 2010, ApJ, 2010, 713, 738

Wilson, G. et al. 2004, ApJ, 154, 107

Yan, H., Dickinson, M., Giavalisco, M., Stern, D., Eisenhardt, P.R.M., & Ferguson, H.C., 2006, ApJ, 651, 24

Yan, L., Sajina, A., Fadda, D., Choi, P., Armus, L., Helou, G., Teplitz, H., Frayer, D., & Surace, J. 2007, ApJ, 658, 778

Younger, J. D. et al. 2007, ApJ, 671, 1241

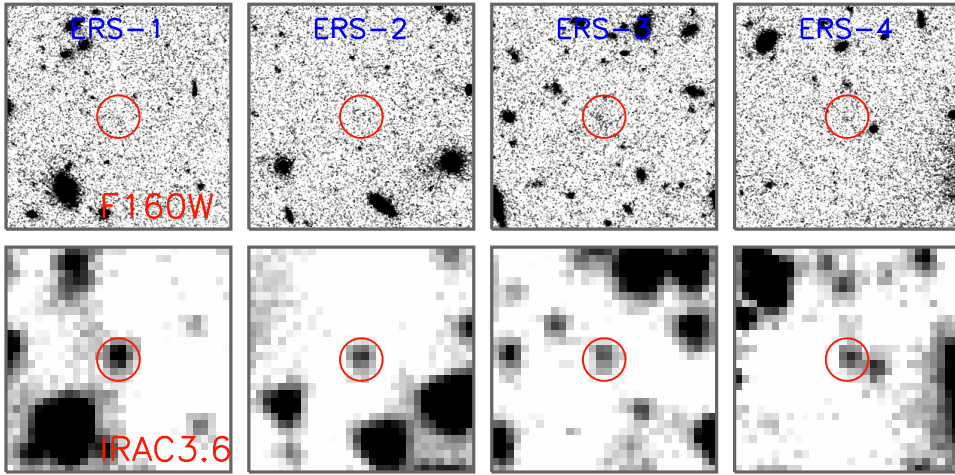


Fig. 1.— Stamp images for the 4 H-band drop-out objects in the GOODS-South field in the F160W and  $3.6\mu\text{m}$  bands. ERS-3 is marginally detected at 24, 250,  $350\mu\text{m}$ , and 20cm. ERS-1 is an X-ray source detected in the Chandra 2Ms imaging (Alexander et al. 2003).

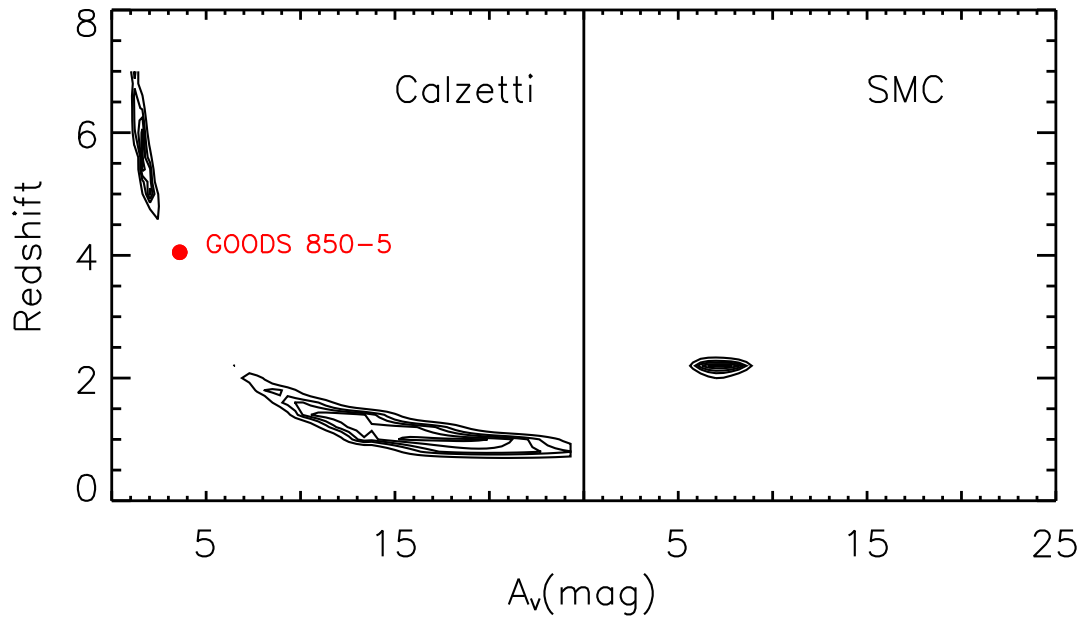


Fig. 2.— The likelihood contours as a function of redshift and dust extinction  $A_V$ . for the best-fit SED of ERS-1. SED fitting for the remaining objects yields the same solutions. The left panel is the contour with the 1Gyr stellar population model and the Calzetti extinction and the right panel with the SMC extinction. The 1Gyr stellar population model with the Calzetti extinction of  $A_V=3.6$  is also the best fit for GOODS 850-5 at  $z=4.05$ .

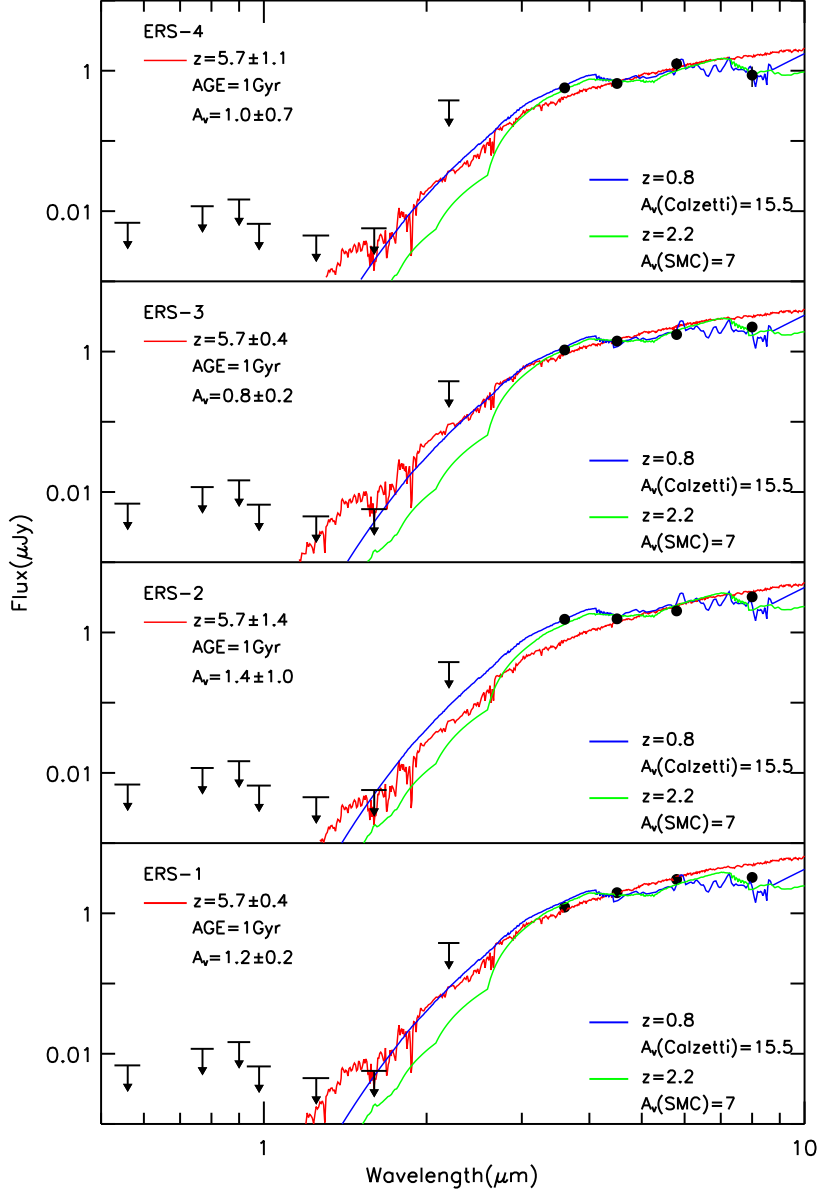


Fig. 3.— Optical-to-MIR SEDs for the H-band drop-out sources in ERS. The best-fit templates to the SEDs are dusty SSP models with  $E(B-V) = 0.2 \sim 0.35$  and  $z_p = 5.7$ . The fitting also yields stellar mass of  $\text{Log}(M_*/M_\odot) = 10.6 \sim 11.2$  for the 4 sources. We also plot two dusty model templates against observed SEDs.

Table 1. Infrared flux densities for the H-band Dropout sources

Name	RA	DEC	F160W	K	3.6 $\mu$ m	4.5 $\mu$ m	5.8 $\mu$ m	8.0 $\mu$ m	24 $\mu$ m
ERS-1	53.084726	-27.707964	0.0066 $\pm$ 0.002	0.2904 $\pm$ 0.1398	1.23 $\pm$ 0.03	1.97 $\pm$ 0.04	3.04 $\pm$ 0.24	3.25 $\pm$ 0.26	-11.7 $\pm$ 3.8
ERS-2	53.132749	-27.720144	0.0036 $\pm$ 0.002	-0.0431 $\pm$ 0.1681	1.54 $\pm$ 0.20	1.56 $\pm$ 0.10	2.03 $\pm$ 0.26	3.21 $\pm$ 0.28	14.7 $\pm$ 4.0
ERS-3	53.060827	-27.718263	0.0019 $\pm$ 0.002	0.0727 $\pm$ 0.1398	1.05 $\pm$ 0.03	1.41 $\pm$ 0.05	1.75 $\pm$ 0.23	2.24 $\pm$ 0.25	39.5 $\pm$ 4.3
ERS-4	53.167161	-27.715316	0.0054 $\pm$ 0.002	0.2628 $\pm$ 0.1382	0.57 $\pm$ 0.06	0.66 $\pm$ 0.06	1.25 $\pm$ 0.25	0.87 $\pm$ 0.28	5.9 $\pm$ 3.6

Note. — All flux densities in this table are in unit of  $\mu$ Jy.